WORLD CONFERENCE ON TIMBER ENGINEERING 2025
BRISBANE, AUSTRALIA
Advancing Timber for the Future Built Environment

THERMAL ANALYSIS OF GLULAM FOR THE DEVELOPMENT OF NEW REDUCTION FACTORS FOR STRENGTH AND STIFFNESS IN FIRE

Katrin Nele Mäger[1], Cvetanka Chifliganec[2], Christoph Kurzer[3], Norman Werther[4], Alar Just[5], Andrea Frangi[6]

ABSTRACT: This paper presents thermal properties based on several unloaded fire tests of glued laminated timber beams with various cross-sections. Temperature measurements from the tests are used to calibrate new effective thermal properties of timber needed for numerical estimation of the mechanical behavior of one-side fire exposed beams loaded in bending. The basic one-dimensional charring rate of the tested beams is determined based on the temperature measurements from the tests and 3D models of the cleaned burnt specimens. Using the calibrated effective thermal properties of timber, the temperature profiles of the cross-sections, as well as the mechanical behavior of one-side fire exposed beams loaded in bending, are successfully numerically simulated.

KEYWORDS: timber, temperature, charring rate, thermal properties, FE analysis

1 - STATE OF THE ART

Focusing on temperature-dependent strength and stiffness reductions, the review of the current state of research shows that the thermo-mechanical properties of timber are crucial for modelling the fire resistance of timber structures. The data from several studies indicate the variability in the reduction factor for strength and stiffness due to differences in experimental setups, timber species, and dimensions of specimens. Also, significant gaps in existing research are experiments on a larger scale, with massive timber elements, the influence of moisture migration, and especially the influence of real fire exposure.

The structural performance of timber elements during a fire is influenced by their mechanical properties, which are inherently temperature-dependent. Unlike materials such as steel and concrete, timber undergoes degradation over a considerably narrower temperature range. Both softwood and hardwood generally experience a significant loss of strength and stiffness—regardless of grain orientation—within the temperature range of approximately 20 – 300°C due to pyrolysis, ignition, and subsequent charring. High-temperature gradients in timber exposed to fire cause significant variations in mechanical properties across the member.

Timber is characterized by its orthotropic nature and strength properties that vary based on species, density, moisture content, stress state, and loading duration. The mechanical properties of natural, unmodified timber are also influenced by its grain orientation, with the wood being strongest and stiffest when the grain runs parallel to the applied load. Structural elements of timber experience primarily compressive or tensile stresses along the longitudinal (parallel to grain) direction. As a result, the existing knowledge and interest is mainly focused on the longitudinal direction. If timber has been heated beyond 300 °C (i.e., charred), its strength cannot be recovered. Timber heated to 100 -300°C can be recovered.

[1] Katrin Nele Mäger, School of Engineering, Tallinn University of Technology, Tallinn, Estonia, ORCID: 0000-0002-6623-9263

[2] Cvetanka Chifliganec, ETH Zürich, Switzerland, cvetanka.chifliganec@ibk.baug.ethz.ch

[3] Christoph Kurzer, Technical University of Munich, Germany, ORCID: 0000-0001-7559-7110

[4] Norman Werther, Technical University of Applied Sciences Augsburg, Germany, ORCID: 0000-0001-9762-1329

[5] Alar Just, Tallinn University of Technology, Estonia, ORCID: 0000-0002-8001-401X

[6] Andrea Frangi, ETH Zürich, Switzerland, ORCID: 0000-0002-2735-1260

https://doi.org/10.52202/080513-0573

There is considerable uncertainty around the mechanical properties of timber at elevated temperatures, with varied values reported in the literature. Properties measured in fire and at heated conditions (without fire) have often been mixed. Many studies have concluded that the significant discrepancies in the strength reductions observed in various tests are likely attributed to the differing experimental setups utilized by different researchers, as well as the inherent variability in factors such as timber grading, moisture migration, creep, etc.

Based on the systematic studies carried out by König in [3,4], a design model for the determination of the residual cross-section of the timber members and a mechanical model providing reduction factors for the mechanical properties of the residual cross-section of timber was proposed by König & Walleij [2]. This considered all the shortcomings of earlier investigations [8,9,10].

The fire test specimens tested by König in 1995 in the model scale furnace consisted of solid timber members with cross-sections 45x95 to 45x195 mm^2 and mineral wool protecting its sides from fire. For each test specimen, the bending strength was predicted for normal temperature conditions. Additionally, full-scale tests were conducted using walls. The test results showed that extensive plastic flow occurred in the timber members, giving rise to the neutral axis being moved toward the unexposed side of the member. This effect was more pronounced when the exposed side of the timber member was in compression. It was argued that the conditions in the wood were to some extent similar to those when applying the technique of steaming for bending of wood, e.g., when manufacturing bentwood for Thonet chair No.14.

Whilst the objective of the study in 1995 was to investigate the fire performance of timber frame assemblies at standard fire exposure (also including three full-scale wall assembly tests), then in 1997, 23 wall tests were carried out on medium scale to show the effect of parametric fire exposure in relation to the standard fire. The studies demonstrated that the residual bending strength agreed relatively well with the results published in the pilot study by König (1995).

As stated in the report by König & Walleij, the model developed for determining the strength and stiffness parameters used temperature values obtained as output from heat transfer calculations and reduced material properties of strength and modulus of elasticity for tension and compression. The obtained reductions of properties included the effect of moisture, time, and mechano-sorptive creep, all of them being important, especially in a temperature range around 100 °C. Modification factors for the fire were calculated, giving the reduction of strength and stiffness properties of the residual cross-section. The properties were calculated by dividing the timber cross-section into small elements and using local strain-stress relationships with temperatures obtained in the heat transfer calculations. With the simplified bilinear stress-strain relationship as a starting point from Buchanan in 1990 [11], relationships were determined of compressive strength, tensile strength, and modulus of elasticity versus temperature and reported in CIB-W18 [12].

König & Walleij [2] have pointed out that Thomas [9] evaluated the test results by König in 1995 [3] and simulated these conditions by assuming a decrease of the localized compressive strength in the region of 100 °C, while the reduction of tensile strength was less. Corresponding reductions of the modulus of elasticity, as used by Thomas, are shown in Figure 2.

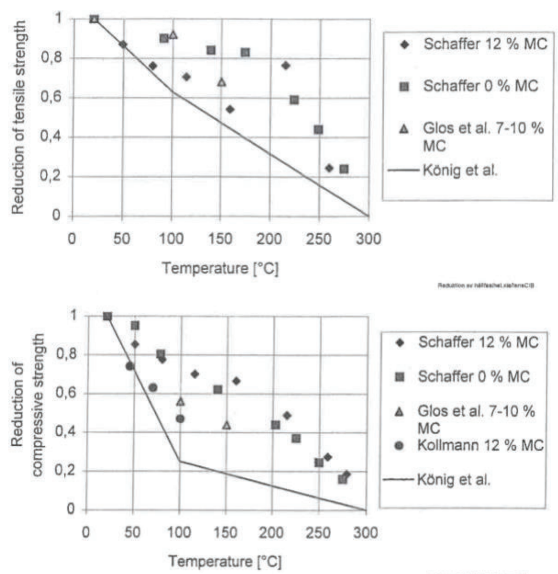

Figure 1. Effect of temperature on tensile strength (upper) and compressive strength (lower), obtained from the paper by König & Walleij, CIB-W18 [12].

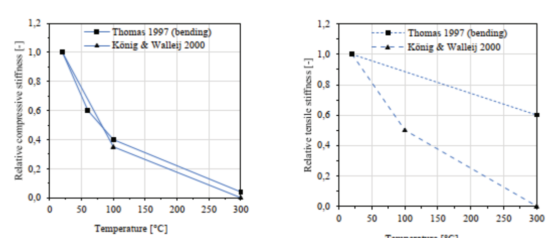

Figure 2. Comparison of reduction in compressive (left) and tensile (right) stiffness between the two studies (experimental and numerical).

https://doi.org/10.52202/080513-0573

2 – MEDIUM SCALE FIRE TESTS

Medium-scale fire tests were performed at ETH Zurich, using the novel custom-built fire simulator from June to August 2023. All members from the test program were made of glulam with vertical 40 mm tick lamellae without finger joints in the heated region. All boards were machine strength graded with a narrow density range (435-513 kg/m3) to provide test specimens with well-known and similar mechanical properties. The thermocouples for each test specimen were installed at several positions through the height of the cross-section and at three different measuring stations through the length. The temperature measurements obtained from the tested specimens were utilized as a foundation for finite element analysis and developing new temperature-dependent mechanical properties of timber.

2.1 Fire simulator

The medium-scale fire tests were carried out in a fire simulator with a fire chamber of 1 m x 1.67 m x 1 m. The temperature control is done by 10 gas burners and 12 plate thermometers. The fire simulator is equipped with a 100-channel thermocouple Data Acquisition system (DAQ) box, of which two are almost always used for room ambient temperature measurement.

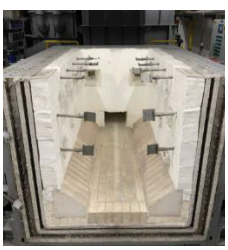
a)


b)

Figure 3. Fire simulator a) with open fire chamber b) fire chamber closed with lids for a beam test

2.2 Test specimens

Test specimens were produced in Rubner Holz. All glulam beams were made with vertical lamellas for testing in the horizontal position. Timber members with four cross-section sizes were tested: 80x80 mm, 80x160 mm, 160x160 mm, and 240x240 mm.

Thermocouples were installed at three locations along the length of the beam (see Figure 4). The locations are marked with letters A, B, and C and green dashed lines. The part of the beam shown between the red dashed lines is exposed to fire from below.

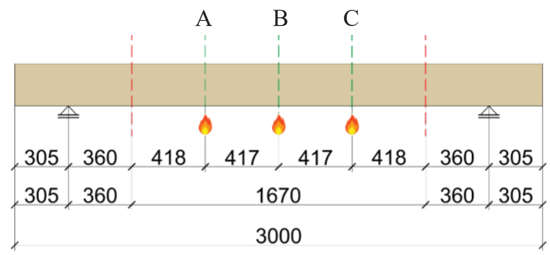

Figure 4. Location of thermocouple stations

Each thermocouple station had multiple thermocouples installed at different depths from the fire-exposed side.

The planned locations for thermocouples at each station for unloaded fire tests are shown in Figure 5. Fire exposure is considered from below. The numbering of thermocouples starts from the fire-exposed side.

Type K thermocouples were used, and the wires were twisted together by about 5 mm at the ends. Holes with a diameter of 2 mm were drilled to the prescribed locations. Thermocouples were installed before gluing. To ensure proper adhesion, grooves were routed into the lamella with the thermocouples, and multiple wires were placed into the groove (see Figure 6).

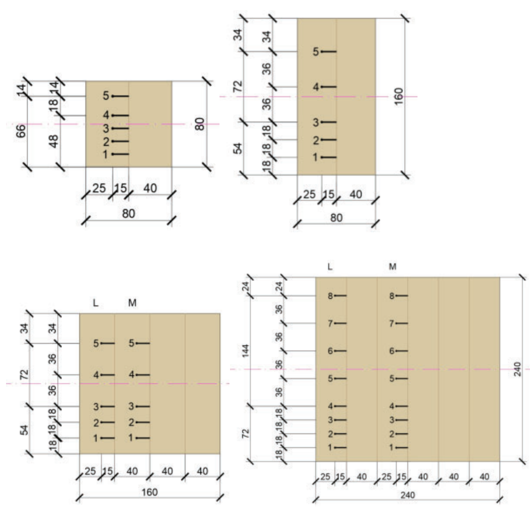

Figure 5. Thermocouple locations

Figure 6. Grooved lamella with thermocouples

After the installation of thermocouples, the lamellae were prepared to be glued in the production line. Great care was taken to protect the thermocouple wires from damage during gluing and planing (see Figure 7). This was done by staggering the length of the lamellas, with the instrumented lamella being the longest. Once all specimens were glued and the appropriate hardening and curing time had passed, they were planed to their final dimensions.

The actual locations of thermocouples were determined. Before planing, pilot holes with a specific depth were drilled to different locations on the beams. After planing, the depth reduction was measured, and the new thermocouple locations were determined.

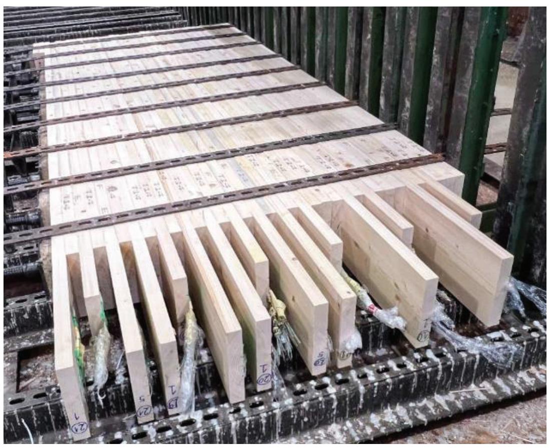

Figure 7. Specimens after glue application in presses

To ensure the fire exposure is one-sided, side protection was applied to the vertical sides of all beams, as shown in Figure 8. The protection consisted of 20-mm thick timber board strips covered by 15-mm thick gypsum board strips. The joints between strips were stacked. The protection boards were attached by high-temperature resistant sealant and screws. 1-2 mm gaps were left between the strips to reduce the possibility of their interference with the load-bearing behavior (deflections) in further loaded tests.

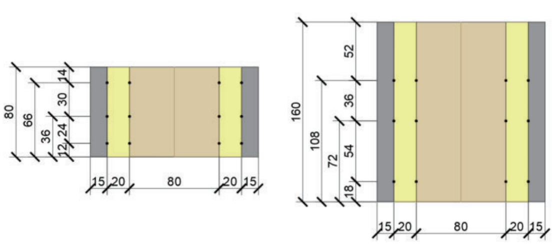

Figure 8. Side protection schematic (grey: gypsum board, yellow: wood)

Figure 8 shows the locations of thermocouples installed between the protection boards and the beams as black dots. For the 80x80 mm cross-section, the distances of the thermocouples from the fire-exposed surface were 12, 36, and 66 mm. For all other cross-sections, the thermocouples were located at 18, 72, and 108 mm from the fire-exposed surface.

2.3 Test procedure

The tests followed the ISO 834 standard time-temperature exposure controlled automatically by plate thermometers in the furnace.

The tested beam was placed horizontally on top of the furnace (see Figure 9). Two special side lids covered the rest of the top opening of the furnace. Any gaps were tightened with ceramic and stone wool.

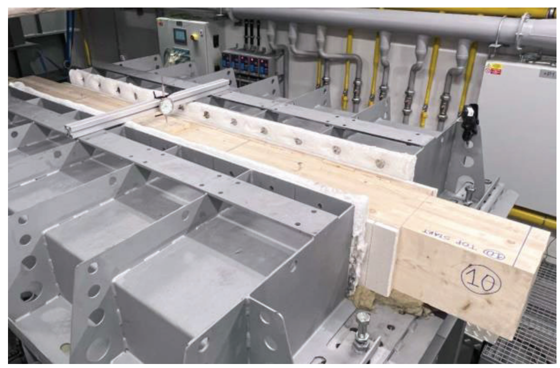

Figure 9. Specimen set up for testing

The specimen was exposed to the standard fire for 30, 60, or 90 minutes. The thermocouple wires were cut a few minutes before the prescribed fire exposure time was reached. The burners were switched off immediately before the specimen was lifted from the furnace. The specimen was extinguished using water.

Figure 10. Specimen after testing and extinguishment

https://doi.org/10.52202/080513-0573

2.4 Test results

The maximum and average temperatures are presented in the following graphs. The average temperature was calculated for the same depth of thermocouples at each station per specimen.

Three tests were performed with each cross-section. Figure 11 shows the average and maximum temperatures of tests with an 80x80 mm cross-section. The three tests showed very good repeatability. Figure 12 and Figure 13 show the average and maximum temperatures in the left and middle lamella of the 240x240 mm cross-sections, respectively. The difference between the average and maximum temperatures per specimen and between three tests is bigger than for smaller cross-sections.

However, for the middle lamella, the variation is small. In the left lamella (Figure 12), the time to reach charring at 18 mm varies between 28 to 32 minutes, the time to reach charring at 36 mm varies between 52 to 58 minutes, and the time to reach charring at 54 mm varies between 78 to 90 minutes. In the middle lamella (Figure 13), the time to reach charring at 18 mm is after 30 minutes without variation, the time to reach charring at 36 mm varies between 54 to 57 minutes, and the time to reach charring at 54 mm varies between 85 to 88 minutes.

The effectiveness of the side protection is shown in the temperature measurement graphs below. In all following graphs, "Gyp" signifies the thermocouples behind the gypsum boards, i.e., between gypsum and timber protection. "Lam" denotes thermocouples between the test specimen and the protection boards.

Figures 14 and 15 show the temperatures measured on the sides of the specimens and behind the protective boards for all specimens. See Figure 8 for the placing of thermocouples.

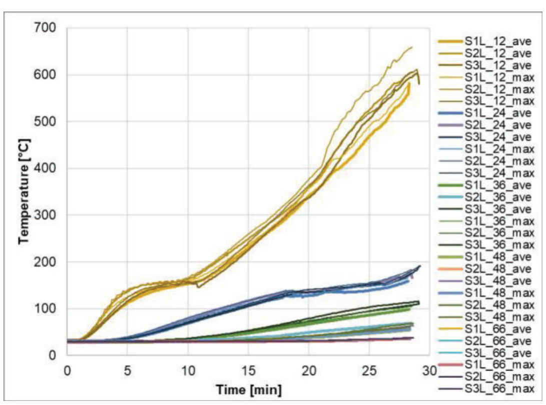

Figure 11. Tested average and maximum temperatures in 80x80 specimen

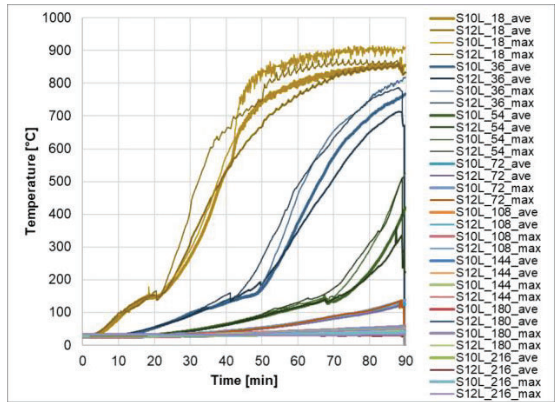

Figure 12. Tested average and maximum temperatures in the left lamella of 240x240 specimen

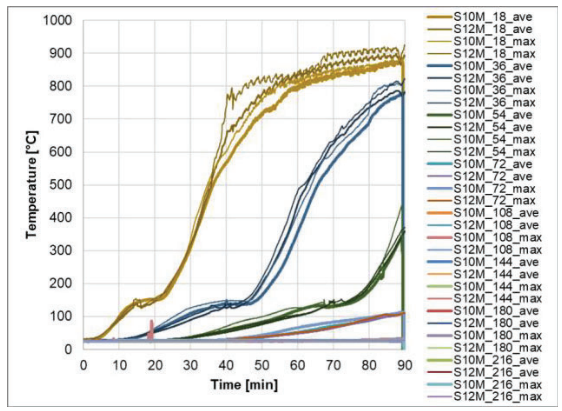

Figure 13. Tested average and maximum temperatures in middle lamella of 240x240 specimen

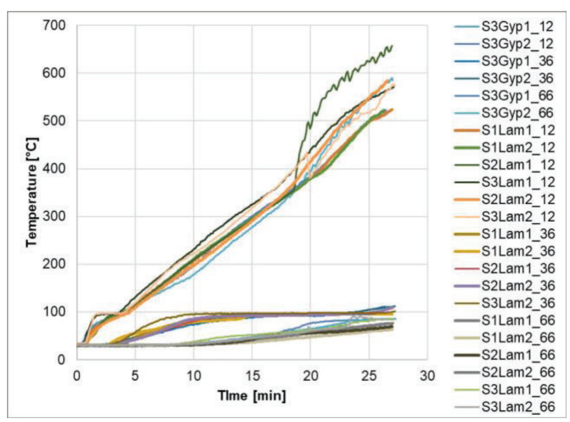

Figure 14. Tested temperatures in protection of 80x80 specimen

For the 80x80 specimens, the temperatures inside and behind the protection are similar except for one of the thermocouples on the side of specimen 2 at 12 mm (see Figure 14). For the 240x240 specimens, the temperatures inside and behind the protection are similar (Figure 15).

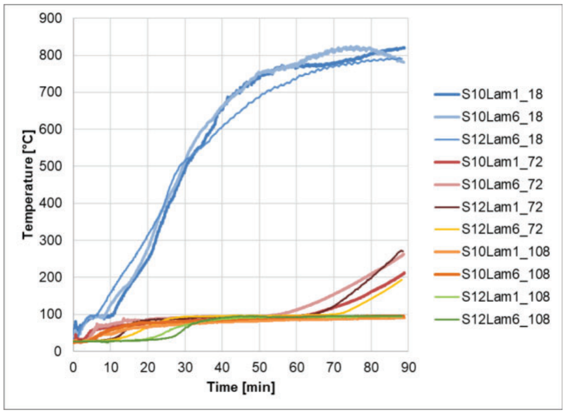

Figure 15. Tested temperatures in protection of 240x240 specimen

2.5 Charring rates

Charring rates from unloaded fire tests were analyzed based on thermocouple measurements. The actual locations of thermocouples were used to calculate the charring rate. The times to reach 300 °C at each thermocouple were recorded. The summary of charring rates per specimen size is presented in Table 1.

Table 1. Charring rates of unloaded fire test specimens

Cross-section	Average charring rate (mm/min)
80x80	0,66
80x160	0,63
160x160	0,62
240x240	0,66

The unloaded fire tests showed good repeatability. Charring was kept mostly one-dimensional by the applied side protection. The charring rates measured by thermocouples were, on average, compatible with the Eurocode value. The unloaded fire tests provide a solid basis for further activities within the project.

3 – THERMAL FE-ANALYSIS

Temperature data was compared to thermal simulations. These tests aimed to gather data about the temperature distribution and development within the specimen. The temperature data of the unloaded fire tests showed similar results and allowed to model the isotherms in three sections. The side protection was also implemented in the simulations. See Figure 16.

Symmetry along the vertical axis through the middle of the specimen was used in the simulations, also to reduce the time required to run the simulations.

All specimens from unloaded fire tests were simulated using the appropriate input parameters described in Table 2.

Table 2. Mesh size in thermal simulations

Cross-section (bxh)	Specimen number	Mesh Size (bxh)		
		Zone 1	Zone 2	Zone 3
80x80	1,2,3	1x1	1x1	1x1
80x160	4,5,6	1x1	1x1	1x1
160x160	7,8,9	1x1	3x1	3x1
240x240	10,11,12	1x1	3x1	6x1

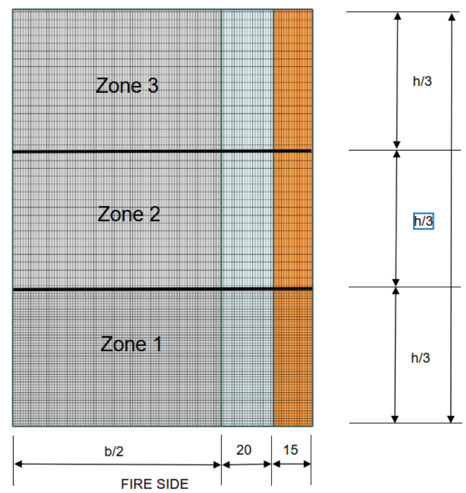

Figure 16. Simulated cross-section. Mesh and dimensions.

Boundary conditions in the simulations were implemented similarly in all four specimen sizes. Figure 17 shows the boundary conditions used in thermal simulations by the example of an 80x80 cross-section. The fire exposed surface was exposed to the ISO 834 standard fire (red line). The vertical surfaces were adiabatic (black lines), with the left one being an axis of symmetry (black dash-dot line). The unexposed surface was given a boundary temperature of 20 °C (blue line). Timesteps of 5 seconds were used in the thermal simulations. A precision value of 0.002 was used.

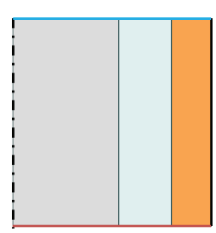

Figure 17. Boundary conditions exemplified on 80x80 cross-section

https://doi.org/10.52202/080513-0573

The convection coefficient for heated surfaces was taken as 25 W/m²K and 4 W/m²K on unheated surfaces according to EN 1991-1-2 [13]. Emissivity was considered 0.8 according to EN 1995-1-2 [14].

SAFIR calculates the heat transfer in solids as conduction. All construction materials are described as solids. Thermal conductivity, specific heat capacity, and density change at elevated temperatures. Table 3 shows the thermal properties of timber according to FprEN 1995-1-2 [1]. The densities of unloaded specimens were measured before the tests and were used as the densities at 20 °C (ρ20) for calculating the reduction of density. The densities of specimens were between 435 and 513 kg/m^3. The average temperatures recorded in unloaded fire tests were used for comparison with simulations since simulations should capture the average temperature response of a timber element and cannot capture imperfections and extremes (e.g., big knots and cracks).

Table 3. Thermal properties of timber according to EN 1995-1-2

Temperature [°C]	Thermal conductivity [W/(mK)]	Specific heat [J/(kgK)]	Density ratio ρ/ρ20 [-]
20	0.12	1530	1.00
99	0.13	1770	1.00
100	0.13	13600	1.00
120	0.14	13600	1.00
121	0.14	2120	0.89
200	0.15	2000	0.89
250	0.12	1620	0.83
300	0.10	710	0.68
350	0.07	850	0.46
400	0.08	1000	0.34
500	0.09	1200	0.30
600	0.18	1400	0.25
800	0.35	1650	0.23
1200	1.5	1650	0

The main focus was given to capturing temperatures below 300 °C. This temperature range is relevant to subsequent analysis of the mechanical performance, as according to the new Eurocode 5 Part 1-2 [1], the reduction factors are considered zero at higher temperatures.

The comparison of test averages and thermal simulations for the 80x80 mm cross-section, specimens 1, 2, and 3, is shown in Figure 18. It is evident that the standard thermal properties underestimate the temperature development in the lower range and slightly overestimate higher temperatures. For the purpose of design of timber structures, where the standard thermal properties should represent the average charring behavior, this result is acceptable. However, for the further analysis of the loaded tests conducted within this project, the temperature range below 300 °C is most relevant.

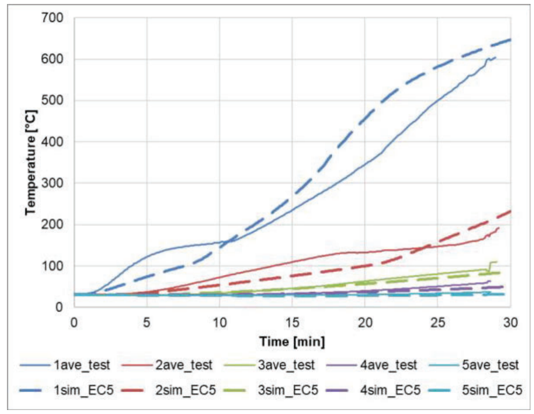

Figure 18. Comparison of simulations with standard thermal properties with test averages for tests 1,2,3 (80x80 mm)

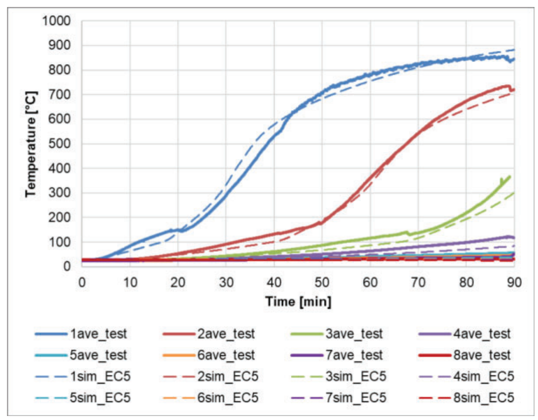

Figure 19. Comparison of simulations with standard thermal properties and test averages for left lamellae of tests 10 and 12 (240x240 mm)

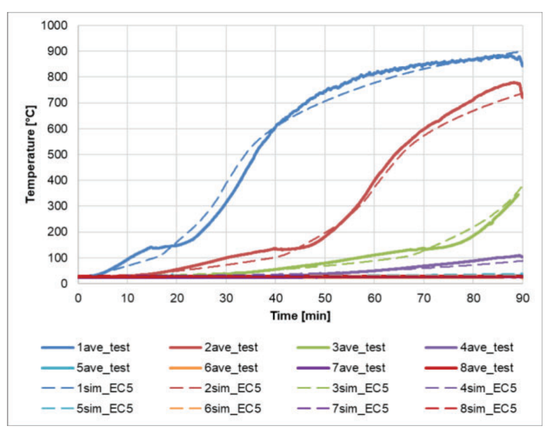

Figure 20. Comparison of simulations with standard thermal properties and test averages for middle lamellae of tests 10 and 12 (240x240 mm)

https://doi.org/10.52202/080513-0573

A similar tendency of underestimation of temperatures below 300 °C can be seen by comparison of test averages and simulations with standard thermal properties of the 80x160 mm cross-section. The comparison of test averages and simulations with standard thermal properties of the 240x240 mm cross-section (specimens 10 and 12) is shown in Figures 19 and 20.

As seen from Figures 18 to 20, the simulations using the thermal properties from the Eurocode did not adequately capture the temperature field in the unloaded fire tests at temperatures below 300 °C. The following describes the procedure undertaken to modify the input parameters of thermal simulations for their result to be closer to test measurements.

A MATLAB script was utilized to manage and analyze the vast data from both tests and simulations and to change the input parameters for the latter. Both thermal conductivity and specific heat values were calibrated. The working principles of the script are described in the following.

The standard thermal properties underestimate the rise in the temperature in the timber element at temperatures below 300 °C, therefore, that range was taken as the basis for the calibration of thermal properties. The average temperatures measured in the unloaded tests and the simulation results at the same location were compared. The script would calculate the mean square error (MSE) and store it in a separate matrix along with the thermal properties.

The script would change one value at a time (e.g., thermal conductivity) by a given percentage and run a new simulation with the changed value. Then, the new MSE would be calculated. This iteration of changing one value and running the simulation to get the new MSE would be looped for all temperatures where the thermal property value is known. Based on the values with the smallest MSE value, the new calibrated properties were found.

The resulting thermal properties are presented in Table 4.

The comparison of thermal conductivity from FprEN 1995-1-2:2025 and calibration results is presented in Figure 21. The calibrated thermal conductivity is slightly higher in temperatures below 300 °C and lower for temperatures above 800 °C than the standard values.

The comparison of specific heat capacity from FprEN 1995-1-2:2025 and calibration results is presented in Figure 22. The calibrated specific heat is relatively similar to the standard values. Minor adjustments have been made to the values below 200 °C and above 450 °C where the calibrated values are lower than the standard.

Table 4. Thermal properties of timber calibrated to fit unloaded fire tests

Temperature [°C]	Thermal conductivity [W/(mK)]	Specific heat [J/(kgK)]	Density ratio ρ/ρ20 [-]
20	0.12	900	1.00
99	0.1056	1331	1.00
100	0.1399	1101	1.00
120	0.1817	11757	1.00
121	0.2763	13905	0.89
200	0.2648	2701	0.89
250	0.2119	1462	0.83
300	0.1856	924	0.68
350	0.1063	903	0.46
400	0.0620	1120	0.34
500	0.0644	1142	0.30
600	0.0744	1897	0.25
800	0.3301	1887	0.23
1200	1.269	1997	0

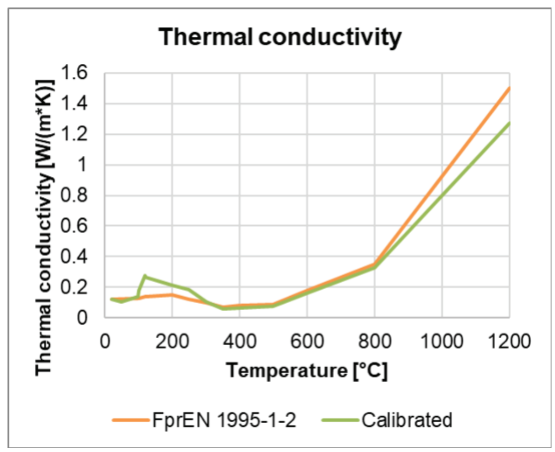

Figure 21. Comparison of calibrated and standard thermal conductivity

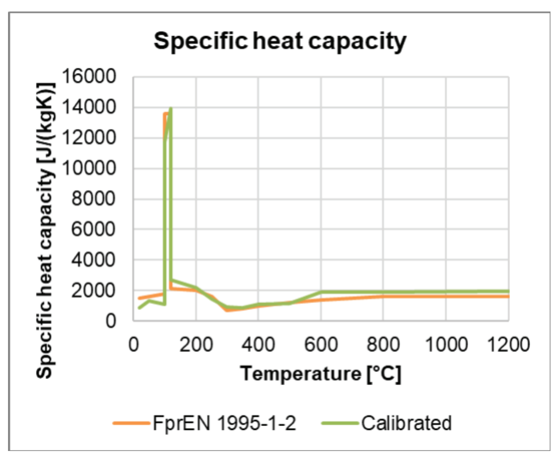

Figure 22. Comparison of calibrated and standard specific heat capacity

https://doi.org/10.52202/080513-0573

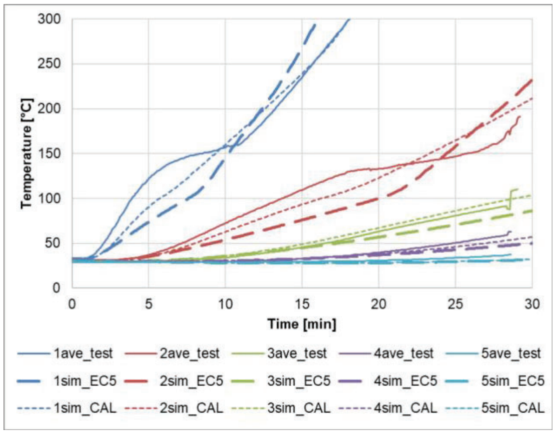

Figure 23. Comparison of simulations with calibrated and standard thermal properties for tests 1,2,3 (80x80 mm)

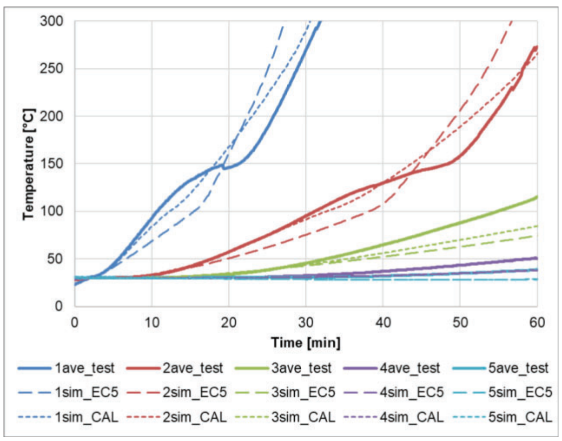

Figure 24. Comparison of simulations with calibrated and standard thermal properties for tests 4,5,6 (80x160 mm)

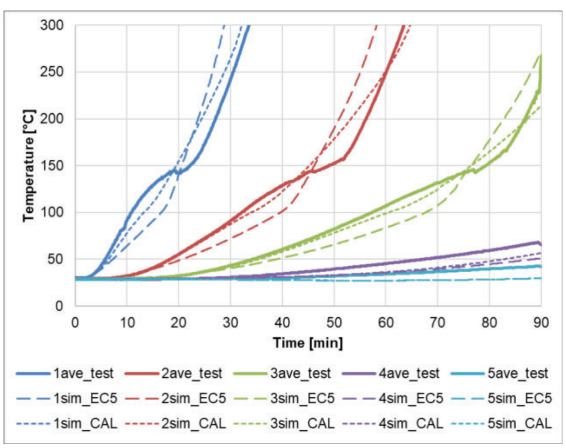

Figure 25. Comparison of simulations with calibrated and standard thermal properties for tests 7,8,9 (160x160 mm)

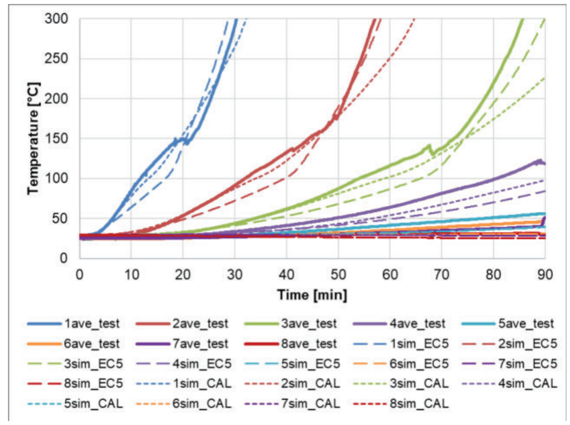

Figure 26. Comparison of simulations with calibrated and standard thermal properties for left lamellae of tests 10,12 (240x240 mm)

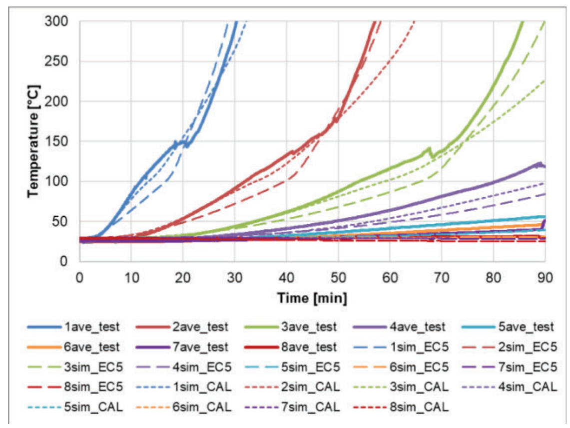

Figure 27. Comparison of simulations with calibrated and standard thermal properties for middle lamellae of tests 10,12 (240x240 mm)

The comparison of thermal simulations with calibrated and standard thermal properties of all cross-sections is shown in Figures 23 to 27. The test averages are shown in a continuous line, the simulations with standard properties in a long dashed line, and simulations with calibrated properties in a narrow dashed line. The temperature range up to 300 °C is highlighted showing that the calibrated properties are able to capture the temperatures more closely to the test averages.

Solid elements were used to model the cross-section of the GL beams. The cross-sections were modeled with a regular mesh with quadrilateral square elements with dimensions of 1 x 1 mm. Depending on the size of the cross-section, different numbers of nodes and finite elements (FE) were used to model the cross-section of the composite GL beams. The 80x160 mm cross-section was modeled with 12800 FE, the 160x160 mm cross-section with 25600 FE, and the 240x240 mm cross-section with 57600 FE.

The influence of the moisture content and density on the charring rate was considered in the numerical models. For each cross-section modeled, the corresponding mean density and moisture content from the bending fire tests with the compressed side exposed to the fire were considered. To simplify the NA, an adjusted density to 12% MC was used. The adjusted density was calculated following the recommendation of EN 384:2016+A2:2022. The results from the thermal analyses are presented in Figures 28 and 29. The temperature profiles of the cross-sections are shown for characteristic times of fire exposure depending on the fire resistance of the specimens.

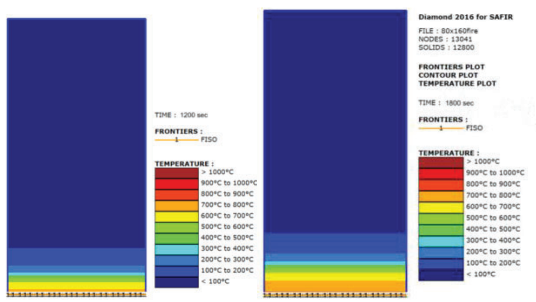

Figure 28. Temperature profile of a 80x160 mm cross-section for a) t= 20 min b) t=30 min

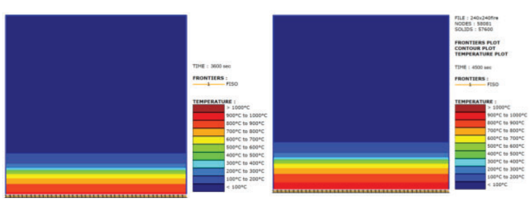

Figure 29. Temperature profile of a 240x240 mm cross-section for a) t= 60 min b) t=75 min

4 – CONCLUSION

The calibrated thermal properties from this study are more accurate in capturing the temperature field in the timber cross-section at temperatures below charring. The thermal properties from the current Eurocode 5 slightly underestimate the rise in temperature below 300 °C. This range is the most relevant as the basis for further thermo-mechanical FE analysis.

5 – REFERENCES

[1] prEN 1995-1-2, "Eurocode 5 - Design of timber structures - Part 1-2: Structural fire design," Brussels, Belgium: CEN, September 2023.

[2] J. König, L. Walleij, "Timber frame assemblies exposed to standard and parametric fires – Part 2: A design model for standard fire exposure," Swedish Institute for Timber Technology Research, Rapport I 0001001, Stockholm, 2000.

[3] J. König, "Fire resistance of timber joists and load-bearing wall frames," Swedish Institute for Timber Technology Research, Rapport I 9412071. Stockholm, 1995.

[4] J. König, J. Norén, F. Bolonius Olesen and F. Toft Hansen, "Timber frame assemblies exposed to standard and parametric fires – Part 1: Fire tests," Swedish Institute for Timber Technology Research, Rapport I 9702015. Stockholm, 1997.

[5] J. König, "Structural fire design according to Eurocode 5 - Design rules and their background," Fire Mater. 29:147–163, 2005.

[6] J.M. Franssen, "SAFIR: A thermal-structural program for modeling structures under fire," Engineering Journal, Vol. 42 No. 3, pp. 143-158, 2005.

[7] K. N. Mäger, D. Brandon and A. Just, "Determination of the effective material properties for thermal simulations," INTER 2016.

[8] Schaffer, E. L., Woeste, F. E. Reliability Analysis of Fire-Exposed Light-Frame Wood Floor Assemblies, Research Paper FPL 386, Forest products Laboratory, US Departmant of Agriculture, USA, 1981.

[9] Thomas, G. C. (1997) Fire resistance of light timber framed walls and floors. University of Canterbury, Canterbury, New Zealand, 1997.

[10] Clancy, P. Time and probability of failure of timber framed walls in fire. PhD thesis, Victoria University of Technology, Australia, 1999.

[11] Buchanan, A. H. (1990) Bending strength of lumber. Journal of Structural Engineering, Vol.116, No. 5.

[12] Konig, J. (2000), A design model for load-carrying timber frame members in walls and floors exposed to fire. CIB Wl8, Paper 33-16-2.

[13] EN 1991-1-2 (2024). Eurocode 1: Actions on structures - Part 1-2: General actions - Actions on structures exposed to fire. Brussels, Belgium: CEN.

[14] EN 1995-1-2 (2004). Eurocode 5: Design of timber structures - Part 1-2: General – Structural fire design. Brussels, Belgium: CEN.

[15] EN 384:2016+A2:2022 (2022). Structural timber - Determination of characteristic values of mechanical properties and density. Brussels, Belgium: CEN.

https://doi.org/10.52202/080513-0573